power can be calculated using the Friis transmission equation [4]. Fig. 3 shows the oscillation frequency, output power and DC-to-RF efficiency as a function of bias voltage V_{ds}. The DC-to-RF efficiency maximum of 24.1% was obtained at V_{ds} = 1.4V. At this bias point, 2.43mW output power was obtained at 14.50GHz with a tuning sensitivity of 120MHz/V. The tuning range of the active antenna was 200MHz. The maximum output power was 9.4mW at V_{ds} = 4.0V.

Conclusions: A new active antenna structure has been presented. The active antenna consists of half wave dipole above the ground plane and a high electron mobility transistor (HEMT). The antenna structure is equivalent to a half wave microstrip dipole antenna with dielectric constants of unity. An output power of 2.43mW with 24.1% efficiency was measured at 14.5GHz. The active antenna should have applications in millimetre-wave power combining using a high-Q resonator.

Acknowledgments: The author would like to thank I. Huhtinen for measuring the electrical performance of the active antenna.

5 July 1994
Electronics Letters Online No: 19941100

O.-P. Lundén (*Technical Research Centre of Finland (VTT), VTT Information Technology, PO Box 1202, Otakaari 7 B, Espoo, FIN-02044 VTT, Finland*)

References

1 CHANG, K., and SUN, C.: 'Millimeter-wave power-combining techniques', *IEEE Trans.*, 1983, **MTT-31**, (2), pp. 91–107
2 THOMAS, H.J., FUDGE, D.L., and MORRIS, G.: 'Gunn source integrated with microstrip patch', *Microwaves & RF*, 1985, **24**, (2), pp. 87–90
3 BIRKELAND, J., and ITOH, T.: 'Spatial power combining using push-pull FET oscillators with microstrip patch resonators'. IEEE MTT-S Dig., 1990, pp. 1217–1220
4 NAVARRO, J.A., HUMMER, K.A., and CHANG, K.: 'Active integrated antenna elements', *Microwave J.*, 1991, **34**, (1), pp. 115–126
5 LEVERICH, W.K., WU, X.-D., and CHANG, K.: 'New FET active notch antenna', *Electron. Lett.*, 1992, **28**, (24), pp. 2239–2240
6 CAMILLERI, N., and BAYRAKTAROGLU, B.: 'Monolithic millimeter-wave IMPATT oscillator and active antenna', *IEEE Trans.*, 1988, **MTT-36**, (12), pp. 1670–1676
7 NAVARRO, J., FAN, L., and CHANG, K.: 'Novel FET integrated inverted stripline patch', *Electron. Lett.*, 1994, **30**, (8), pp. 655–657
8 YORK, R.A., MARINTEZ, R.D., and COMPTON, R.C.: 'Active patch antenna element for array applications', *Electron. Lett.*, 1990, **26**, (7), pp. 494–495
9 CHANG, K., HUMMER, K.A., and GOPALAKRISHNAN, G.K.: 'Active radiating element using FET source integrated with microstrip patch antenna', *Electron. Lett.*, 1988, **24**, (21), pp. 1347–1348
10 YOO, T.-W., and CHANG, K.: '35GHz integrated circuit rectifying antenna with 33% efficiency', *Electron. Lett.*, 1991, **27**, (23), pp. 2117–2118
11 BERMÚDES, L.A., GUILLON, P., OBREGON, J., and BERT, A.: 'A 94GHz low noise GaAs FET oscillator using whispering-gallery dielectric resonator modes and a new push-push configuration reducing 1/f converted noise'. IEEE MTT-S Dig., 1988, pp. 481–483

Optimal boresight error design of radomes of revolving symmetry

F. Hsu, K.K. Chan, P.R. Chang and S.H. Chao

Indexing terms: Radomes, Optimisation, Simulated annealing

An optimisation technique is applied to the design of three-dimensional radomes of revolving symmetry. A design example for an ogive radome is given. The best possible thickness profile of the radome is found and the boresight error is reduced significantly. Both B-spline modelling and polynomial modelling for the thickness profile are considered.

Introduction: In a previous paper [1] we presented a systematic optimisation approach toward radome design. The problem was formulated as a global optimisation procedure such that the boresight error (BSE) of the radome is minimised over the antenna's scan volume by properly adjusting the thickness of the radome layer over the radome surface. In [1] a two-dimensional example was given to show the effectiveness of the approach. In this Letter we consider the design of three-dimensional radomes of revolving symmetry excited by an antenna of uniform current distribution over a circular disk. Such a structure finds many practical applications and is worth considering in more detail.

Optimal design algorithm: The general procedure for the optimal radome design as presented in [1] comprises the following steps. First the thickness profile d as a function of the position on the radome surface is parameterised via the B-spline surface representation. For radomes of revolving symmetry, the surface can be represented in terms of its generator. Accordingly,

$$d(s) = \sum_{i=1}^{N} \beta_i B_i(s)$$

where s denotes the parametric curve length of the generator which, for convenience, is normalised to 1. B_is are the spline basis functions and β_is are the expansion coefficients which remain to be determined through the optimisation process. Next the maximum of the BSE Δ is sought in the antenna's scan volume. The objective is then to search for the best possible βs, and thus the thickness profile $d(s)$, such that the maximal BSE in the antenna's scan volume is minimised, or formulated mathematically:

$$\min_{\beta_1, \beta_2, \ldots, \beta_N} \max_{\theta} \delta(\theta, \beta_1, \beta_2, \ldots, \beta_N).$$

The problem is then reduced to a standard form of global optimisation. The popular simulated annealing technique [2] is employed, which is a statistical search algorithm used in global optimisation problems.

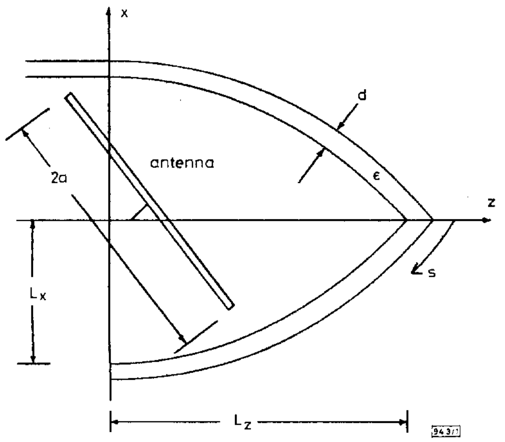

Fig. 1 *Cross-sectional view of three-dimensional antenna-radome system*

Radomes of revolving symmetry: Fig. 1 depicts a general radome of revolving symmetry and its cross-sectional view. The antenna is assumed to be a uniform current distribution over a circular disk of radius a. Owing to the symmetry of this configuration it can be shown that maximal BSE occurs in the principal planes for which the antenna is oriented in the forward direction. It therefore results in considerable saving in computation because only BSE scanned in these two planes needs to be calculated in the above minimax algorithm.

(i) *Design of ogive radome*: As a design example we consider the case of a three-dimensional ogive radome whose generating curve is a circular arc. The radome is made of a material with dielectric constant 4. For simplicity the dielectric loss is not included, because it has negligible effect on the BSE [1] for materials used in practice. The operating frequency is 10GHz. L_x = 6λ and L_z = 12λ, where λ is the free-space wavelength. The maximum scan angle of the antenna is assumed to be 45° about the ogive axis.

For the field evaluation, the local plane wave approximation is used, as we found that it yields sufficiently accurate results as compared to the more rigorous spectral integral approach [1]. The incident fields on the inner surface due to a point source current are calculated and employed to find the transmitted fields on the outer surface, with transmission coefficient corresponding to a planar slab. The total transmitted field is then obtained by linear superposition. Once the transmitted fields on the outer surface are found, the radiation fields, and thus the BSE, can be derived by making use of the equivalence principle.

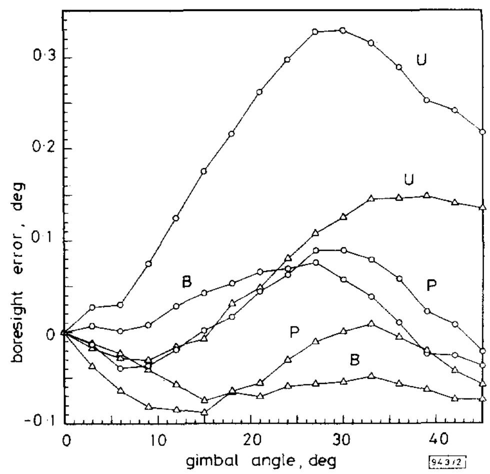

Fig. 2 *Boresight errors for E-and H-plane scans*

U:uniform thickness; B: B-spline modelling; P: Polynomial modelling
○ E-plane
△ H-plane

Fig. 2 shows the boresight errors against gimbal angles for *E*-plane and *H*-plane scans, respectively. In the case of uniform thickness, the BSE has a peak level of 0.33° at an antenna look direction of 30°. After optimisation, it is reduced to 0.075° maximum, a significant improvement as compared to the inherent numerical error of 0.03° when $\epsilon = 1$. The corresponding boresight error rates are also improved. While the boresight error rate can be equally chosen as the objective function to be optimised, we found no appreciable improvement over the above BSE design. The resulting optimal thickness profile function (TPF) is given in Fig. 3.

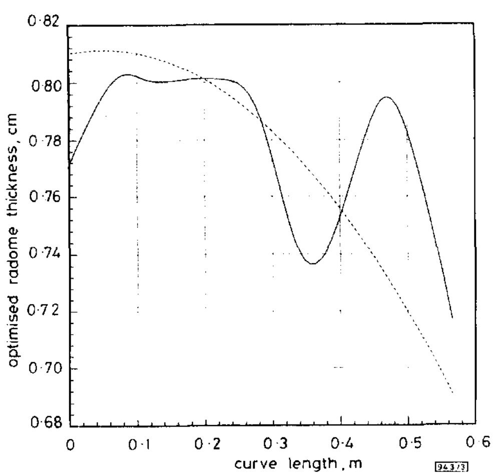

Fig. 3 *Optimised thickness profile functions*

——— B-spline modelling
– – – – polynomial modelling

The optimisation design takes a large amount of computing because it involves many iterative calculations before reaching the desired performances. In our case, it takes about 12000 iterations to reach the desired results. Some data reductions including the curve fitting were employed to save computing time which would otherwise become formidable.

(ii) *TPF modelling by polynomials*: Fig. 3 shows that the optimally designed TPF using the *B*-spline modelling exhibits several excursions over the surface, which makes it undesirable in the precision manufacturing of radomes. Choices other than *B*-spline modelling can be advantageous. Consider the polynomial modelling of the TPF. As a simple case let the generator of the TPF be represented by a polynomial of degree 2 such that

$$d(s) = d_0 + a + bs + cs^2$$

where d_0 is the nominal thickness. a, b, c, as well as the deviation of the thickness from the nominal value $\Delta d = d - d_0$, are allowed to vary in suitable ranges. The solution space is constructed by properly sampling the ranges of a, b, and c. The results for the optimal BSE are shown in Fig. 2. With a peak value of 0.089°, the BSE performance is only slightly degraded as compared to the case of *B*-spline modelling. The polynomial modelling is simple to use, and is more efficient in computation, because only three coefficients are involved. The resulting TPF, as can be seen in Fig. 3, is much smoother as compared to the case of *B*-spine modelling. It varies nearly monotonically and can be machined easily during manufacturing. It should be noted that further improvements can be achieved if higher-order polynomial modelling is employed.

Conclusion: The optimisation method developed previously is applied to the design of three-dimensional radomes of revolving symmetry, where the boresight error is minimised over the antenna scan volume as a result of adjusting the thickness over the radome layer. A design example of an ogive radome is given and the improvement in BSE is significant. Both *B*-spline modelling and polynomial modelling for the thickness profile are considered in the example. It is found that polynomial modelling in such a case yields both a smooth optimal thickness profile and satisfactory BSE performance.

20 July 1994
Electronics Letters Online No: 19941083

F. Hsu, K.K. Chan and P.R. Chang (*Department of Communication Engineering, National Chiao Tung University, Hsinchu, Taiwan, Republic of China*)

S.H. Chao (*Chung Shan Institute of Science and Technology, Lung-Tan, Taiwan, Republic of China*)

References

1 HSU, F., CHANG, P.R., and CHAN, K.K.: 'Optimisation of two-dimensional boresight error performance using simulated annealing technique', *IEEE Trans.*, 1993, **AP-41**, pp. 1195–1203

2 KIRKPATRICK, S., GELATT, C.D., and VECCHI, M.P.: 'Optimisation by simulated annealing', *Science*, 1983, **220**, pp. 671–680

Vertical ground rod (VGR) in inhomogeneous earth of sectoral type

P.D. Rančić, S.Ž. Dzokić and Z.P. Stajić

Indexing terms: Integral equations, Antenna theory, Earthing

The current distribution, line leakage current density and grounding impedance of a vertical ground rod in inhomogeneous earth of sectoral type are presented. This is achieved by using a new system of integral equations.

Introduction: In this Letter, the modified mathematical model of linear antennas [1, 2] in the power frequency domain, is applied to